Rationale Strategy to Tune the Optical Properties of Gold Catenane Nanoclusters by Doping with Silver Atoms

Srestha Basu, Martina Perić Bakulić, Hussein Fakhouri, Isabelle Russier-Antoine, Christophe Moulin, Pierre-François Brevet, Vlasta Bonačić-Koutecký, Rodolphe Antoine

A Rationale Strategy to Tune the Optical Properties of Gold Catenane Nanoclusters by Doping with Silver Atoms

Srestha Basu,[†] Martina Perić Bakulić,[⊥] Hussein Fakhouri,[⊥,†] Isabelle Russier-Antoine,[†] Christophe Moulin,[†] Pierre-François Brevet,[†] Vlasta Bonačić-Koutecký[⊥,¶,§,] and Rodolphe Antoine[†,]**

[†] Univ Lyon, Université Claude Bernard Lyon 1, CNRS, Institut Lumière Matière, F-69622, Lyon, France

[⊥] Center of Excellence for Science and Technology-Integration of Mediterranean Region (STIM), Faculty of Science, University of Split, Ruđera Boškovića 33, 21000 Split, Croatia

[¶]Interdisciplinary Center for Advanced Science and Technology (ICAST) at University of Split, Meštrovićevo šetalište 45, 21000 Split, Croatia

[§] Department of Chemistry, Humboldt Universitat zu Berlin, Brook-Taylor-Strasse 2, 12489 Berlin, Germany

Corresponding Author

Rodolphe Antoine : rodolphe.antoine@univ-lyon1.fr

Vlasta Bonačić-Koutecký: vbk@cms.hu-berlin.de

ABSTRACT. We report the chemical substitution mediated doping of silver atoms into the $Au_{10}SG_{10}$ (SG: glutathione) catenane nanoclusters in a controllable manner. Two levels of doping were conducted leading to two silver-doped $Au_{10-x}Ag_xSG_{10}$ nanoclusters (with x=0-2 and x=1-4). Optical studies reveal that nanoclusters with high level of doping (x=1-4) feature a blue shift in absorption and a significant red shift of ~ 50 nm in the two-photon excited emission spectrum with respect to pristine $Au_{10}SG_{10}$. The preservation of the catenane structure is confirmed by comparing experimental and computational X-ray diffraction patterns and absorption spectra of $Au_{10}SG_{10}$ and its silver-doped analogues. In order to better address the structure-property relationship in such catenane clusters, further theoretical investigations were performed at DFT level. A high-energy shift of the S_1 state is evidenced in the calculated one-photon absorption spectra due to a larger s to d gap in silver caused by smaller relativistic effects in comparison to the gold atoms. Furthermore, the red-shift in the two-photon excited emission band of the clusters is due to significantly larger calculated relaxation of the first excited state in nanoclusters with high level of silver doping.

Introduction

The supramolecular chemistry of gold and, in particular, of gold thiolate leads to fascinating structural motifs with enhanced optical properties.[1] A plethora of synthetic routes have permitted to propose a large number of gold nanohybrid systems ranging from plasmonic gold nanoparticles,[2] atomically precise gold nanoclusters,[3] as well as self-assembled Au-containing thiolated coordination polymers.[4-5] Regarding optical properties, it has been well established in literature that the emission properties of gold nanohybrid systems is strongly dictated by the number and the nature of the metal atoms and the stabilizing ligands.[6-7] Thus, rationale strategies have been proposed to tune the intrinsic emission properties of nanoclusters as a function of their chemical composition. The "doping" strategy stands out as an important one.[8] For instance, doping of gold nanohybrid systems with silver has been demonstrated to lead to enhanced nonlinear optical properties.[9] In context of improving their attractiveness for multiphoton bio-imaging applications, multi-photon excited emission should be pushed further towards the near-infrared window.[10-11]

Silver-doped gold nanoclusters[12] display efficient two-photon excited luminescence[13] and second harmonic conversion.[14] However, for a rational design of nanoclusters with enhanced optical properties, elucidation of the structure-property relationship is of pivotal importance. Doping leads either to preservation or transformation of the nanocluster structure.[7] Furthermore, the correspondence between the optical properties and the heteroatom substitution is still scarcely explored.[15] Shihui Liu[16] conducted a TDDFT study on the excited states and charge redistribution in response to light absorption on single-atom doped Au_{25} nanoclusters, highlighting different absorption features upon Ag, Cu, Pd, and Pt doping. The nature and position of the lowest excited electronic states are also sensitive to silver doping.[17] Other factors like relativistic effects (mainly

due to the Au atoms), the exact spatial position of metal dopants and the heteronuclear Au−Ag bonds have also been reported to affect the fluorescence intensity of gold-doped nanoclusters.[18] From an experimental point of view, developing synthetic routes with atomically precise silver doping of gold nanoclusters with X-ray single crystal resolved structures has largely improved our understanding on these structure–optical property relationship.[19-20]

In this regard, a well-defined structural motif for nanoclusters is an essential prerequisite. We have recently reported a facile "one-pot-one-size" synthesis of $Au_{10}(SR)_{10}$ nanoclusters with SR as glutathione (SG) or thioglycolic acid (TGA).[21-23] The distinct X-ray powder diffraction pattern of $Au_{10}SG_{10}$ was utilized as a signature for homoleptic gold-glutathione catenanes with two Au_5SG_5 interconnected rings.[22] Herein, a rationale strategy for tuning optical properties is reported with chemical substitution by silver atoms doping of $Au_{10}SG_{10}$ catenane system in a controllable manner, leading to silver-doped $Au_{10-x}Ag_xSG_{10}$ nanoclusters with different levels of doping (e.g. x=0-2 and x=1-4). The preservation of the catenane structure is confirmed by comparing experimental and computational X-ray diffraction patterns and absorption spectra of $Au_{10}SG_{10}$ and its silver-doped analogues. DFT study evidences that the ground state geometry changes upon Ag doping are not large. Chiroptical and nonlinear optical properties, i.e. two-photon emission spectra and first hyperpolarizabilities, of silver-doped Au nanoclusters are also reported. Interestingly, these optical studies reveal that $Au_{10-x}Ag_xSG_{10}$ with x=1-4 features a blue shift in absorption and a significant red shift in the two-photon emission spectrum in contrast to $Au_{10}SG_{10}$. A complementary first-principles theoretical analysis has been performed with a focus on the changes of the optical properties of catenane structures upon silver doping.

Methods

Materials: Tetracholoroauric acid ($HAuCl_4.3H_2O$) was purchased from Alfa Aesar. L-glutathione was procured Carl Roth. Methanol, diethyl ether and Silver trifluoroacetate acetate were procured from Sigma Aldrich. All chemicals were used as received without further purification. Ultrapure milli-Q water was used for experimental purpose.

Synthesis of $Au_{10}SG_{10}$: ~ 235 mg of $HAuCl_4.3H_2O$ was added in a round bottom flask and was dissolved in 35 mL methanol using 2 mL triethylamine. To this methanolic solution of glutathione, ~ 100 mg of $HAuCl_4.3H_2O$ was added. The solution was stirred for ~ 24 h. This led to formation of a pale yellow colored solution. To this solution, sodium hydroxide (~ 2 mL) was added till precipitation. The dispersion was centrifuged at a speed of ~ 10,000 rpm for ~ 10 min. The supernatant was discarded and the so obtained pellet was re dispersed in 1 mL of NH_4OH and 2 mL water. This led to complete solubilization of the pellet. The solution was further added with methanol to allow re precipitation. The dispersion was centrifuged for 10 minutes at a speed of 10,000 rpm. The pellet was dissolved in 10 mL water and further added with 1 mL acetic acid. The solution was left undisturbed for ~ 12 h, which led to precipitation of pure $Au_{10}SG_{10}$. The precipitate was collected by centrifugation and was further dissolved in 2 mL water. Re precipitation with methanol was carried out and the so obtained pellet was dried under air for further use.

Synthesis of $Au_{10-x}Ag_xSG_{10}$ with x= 0-2: In order to synthesize $Au_{10-x}Ag_xSG_{10}$ with x= 0-2, a protocol similar to that of $Au_{10}SG_{10}$ was followed – the only difference being that, in the very first step, following addition of $HAuCl_4.3H_2O$ to a methanolic solution of L glutathione, ~ 11 mg of

silver trifluoroacetate (dissolved in minimum amount of methanol) was added to the same solution. The purification process of the doped clusters remained same as that of $Au_{10}SG_{10}$.

Synthesis of $Au_{10-x}Ag_xSG_{10}$ with x= 1-4*:* In order to synthesize $Au_{10-x}Ag_xSG_{10}$ with x= 1-4, a protocol similar to that of $Au_{10}SG_{10}$ was followed – the only difference being that, in the very first step, following addition of $HAuCl_4.3H_2O$ to a methanolic solution of L glutathione, ~ 60 mg of silver trifluoroacetate (dissolved in minimum amount of methanol) was added to the same solution. The purification process of the doped clusters remained same as that of $Au_{10}SG_{10}$.

Gel preparation: ~ 3 g of bisacrylamide and ~ 8.7 g of acrylamide were dissolved in 21 mL of water and was sonicated till complete solubilization. Separately, 49 mg/490 µL of ammonium peroxodisulphate solution was freshly prepared. Further, required amounts of $Au_{10}SG_{10}$ and $Au_{10-x}Ag_xSG_{10}$ with x= 1-4 were dissolved in formerly prepared solution of acrylamide and bisacrylamide to achieve a final concentration of 750 µM in. Thereafter, 1 mL of the solutions containing clusters and doped clusters were added in the gel bath. Following this, 10 µL of TEMED and 10 µL of ammonium peroxodisulphate were added to the gel bath. The system was left undisturbed till complete gelation.

Instrumentation.

Electrospray Ionization Mass Spectrometry (ESI-MS). ESI-MS was performed on a commercial quadrupole time-of-flight (micro-qTOF, Bruker-Daltonics, Bremen, Germany, mass resolution 10 000). The samples were prepared to a final concentration of approximately 50 µM in methanol. The samples were analyzed in negative ion mode; each data pointwas the summation of spectra over 5 min.

UV/Vis and CD spectra are recorded at IBCP Lyon France on a Chirascan spectrometer. CD was carried out on a Chirascan CD (Applied Photophysics). Data were collected at 1 nm intervals in the wavelength range of 200−500 nm at 20 °C, using a temperature-controlled chamber. A 0.01 cm cuvette containing 30 μL of NC sample at 50 μM was used for all the measurements. Each spectrum represents the average of three scans, and sample spectra were corrected for buffer background by subtracting the average spectrum of buffer alone.

X-ray diffraction (XRD) is carried out on a PANalytical EMPYREAN diffractometer with a PIXcel 3D using Cu Kα radiation and a high-resolution theta−theta goniometer.

NLO Measurements. The setup for hyper-Rayleigh scattering (HRS) and two-photon excited fluorescence (TPEF) has been described in detail in previous works.[23-25] HRS measurements was a performed using a modelocked femtosecond Ti:sapphire laser delivering at the fundamental wavelengths between 785 and 810 nm pulses with a duration of about 140 fs at a repetition rate of 80 MHz. A fundamental beam was focused by a low numerical aperture microscope objective into a 0.5 cm spectrophotometric cell containing the aqueous solutions. For the TPEF signal, the wavelength of the spectrometer (Jobin-Yvon, iHR320 spectrometer) was scanned between 350 nm and 750 nm detected with a photomultiplier tube (model H11890-210, Hamamatsu). For reference materials, we have chosen fluorescein dye. From the literature, we assume at the excitation wavelength of 780 nm: σ_2 (fluorescein) = 33.3 GM using a quantum yield of 0.9 and a two photon absorption cross-section of 37 GM. In addition, TPEF measurements were performed on nanoclusters-containing gels with a customized confocal microscope. The luminescence was excited at 780 nm with a mode-locked frequency-doubled femtosecond Er-doped fiber laser (C-Fiber 780, MenloSystems GmbH). The laser spectrum was bounded by two filters (FELH0750 and FESH0800, Thorlabs Inc.). The output power of the femtosecond laser was 62 mW. The laser

beam was focused by a Nikon Plan Fluor Ph1 DLL objective (10x/0.30 NA). The emitted signal was collected in epifluorescence illumination mode. The two-photon fluorescence emission was separated from the incident light through a dichroic mirror (NFD01-785, IDEX Health & Science LLC). A FESH0750 filter (respectively a FELH0800 filter) was used in order to remove the residual photons coming from the excitation laser and collect visible 350-750 nm fluorescence (respectively infrared 800-900 nm fluorecence). The two-photon fluorescence emission spectra were recorded using an iHR320 spectrometer equipped with a 53024 grating from Horiba Jobin Yvon, and detected by a -20°C cooled photomultiplier tube (R943-02, Hamamatsu Photonics).

Computational details

The structural properties have been determined employing DFT method with B3LYP functional[26-28] and split valence polarization (SVP) atomic basis set[29] as implemented in TURBOMOLE 7.4.[30] Optical properties (OPA, TPA, CD and β hyperpolarizabilities) have been determined using TDDFT[31-32] and a quadratic response[33-34] approach as implemented in the DALTON program package.[35-36] The same AO basis set has been used as for structural properties except for the ligands for which 6-31G basis set[37-40] has been employed. In the lowest energy 5,5' catenane structures: $Au_{10}L_{10}$, Au_9AgL_{10} $Au_7Ag_3L_{10}$, L labels the chiral ligand ($-SCH_2CH(NH_2)CH_3$). For gold and silver atoms 19 e^- relativistic effective core potential (19 e^- RECP) taking into account scalar relativistic effects has been employed.[41] The Debye formula serves to calculate XRD patterns.[42]

Results and Discussion

Experimentally, Au_{10} clusters stabilized by glutathione, with molecular formula $Au_{10}SG_{10,}$ were synthesized following a method previously reported by our group.[22] Unambiguous assignment of $Au_{10}SG_{10}$ was achieved by high-resolution electrospray ionization – mass spectrometry (ESI-MS), see **Figure S1** in supplementary file (SI). In the next step, systematic doping of the as-synthesized $Au_{10}SG_{10}$ with silver atoms was performed by adding optimized amounts of silver trifluoroacetate. Details of the doping process are given in SI. Briefly, the strategy of the study is to perform gradual doping of $Au_{10}SG_{10}$ with silver atoms by varying the amount of silver trifluoroacetate reacting with $Au_{10}SG_{10}$. Evidence of doping with silver atoms of the Au_{10} nanoclusters with the appearance of $Au_{10-x}Ag_xSG_{10}$ nanoclusters was obtained from high-resolution ESI-MS, see **Figures S2 and S3** in SI. These syntheses led to a distribution of $Au_{10-x}Ag_xSG_{10}$ systems with x ranging from 0-2 and with x ranging from 1-4 for the two silver-doped gold nanoclusters samples, respectively.

Next, we were interested to investigate the effect of gradual silver doping on the optical and chiroptical properties of $Au_{10}SG_{10}$. As evident from **Figure 1A**, the UV-vis absorption spectrum of $Au_{10}SG_{10}$ features two discernible bands at 331 nm and 369 nm. The UV-vis absorbance spectrum of $Au_{10-x}Ag_xSG_{10}$ with x= 0-2 features slight blue shifted bands at 324 nm and 364 nm respectively. Instead, the UV-vis spectrum of $Au_{10-x}Ag_xSG_{10}$ with x= 1-4 shows a monotonic increase of intensity below 390 nm with no discernable shoulder. Thus, it is observed that systematic doping of $Au_{10}SG_{10}$ with varying number of silver atoms leads to blue shift of the onset of absorption from 410 nm to 390 nm. In an allied vein, and in order to verify whether a similar trend of variation is observed in the chiroptical properties of the ligated Au_{10} clusters as well as

for further corroboration with the UV-vis absorption results, circular dichroism (CD) studies were performed. As can be observed from **Figure 1B**, the CD spectrum of $Au_{10}SG_{10}$ features a strong peak at 326 nm. However, the peaks in the CD spectrum of $Au_{10-x}Ag_xSG_{10}$ with x= 0-2 and x=1-4 were observed to occur at 321 nm and 312 nm, i.e. slightly blue shifted compared to $Au_{10}SG_{10}$ and with decreasing values of ellipticity, see **Figure 1B**.

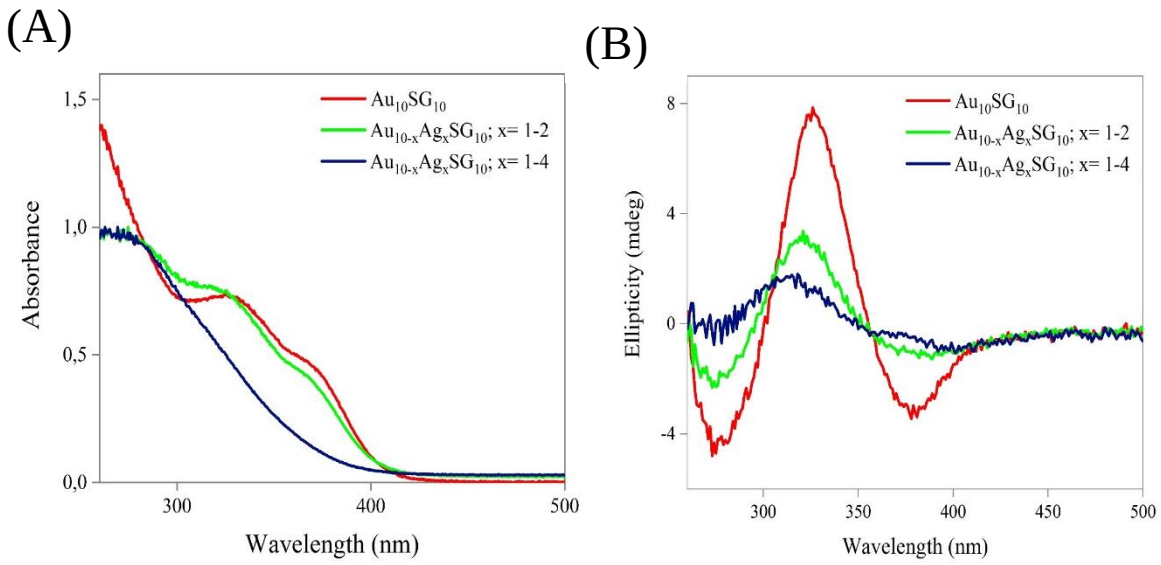

Figure 1: UV−vis absorption and CD spectra of as-synthesized $Au_{10}SG_{10}$, $Au_{10-x}Ag_xSG_{10}$ (x= 1-2) and $Au_{10-x}Ag_xSG_{10}$ (x = 1-4) NCs in aqueous solution.

Under UV light, aqueous solutions of $Au_{10}SG_{10}$ and silver doped nanoclusters showed extremely weak fluorescence. However, in our previous study, it was found that $Au_{10}SG_{10}$ presented large first hyperpolarizability and two-photon excitation fluorescence (TPEF).[22] In the current study, the TPEF emission spectrum of $Au_{10-x}Ag_xSG_{10}$ with x= 1-4 was recorded and compared with that of $Au_{10}SG_{10}$. Notably, the normalized TPEF emission spectrum of $Au_{10}SG_{10}$ features a maximum at 555 nm while the maximum of TPEF emission spectrum of $Au_{10-x}Ag_xSG_{10}$ with x= 1-4 is observed

to occur at 605 nm, see **Figure 2**. Thus doping $Au_{10}SG_{10}$ with silver atoms leads to a significant bathochromic shift of ~ 50 nm. The superimposed (non-normalized) emission spectra of $Au_{10}SG_{10}$ and $Au_{10-x}Ag_xSG_{10}$ with x= 1-4 in gels with a cluster concentration of 750 μM are shown in SI, see **Figure S4**. The TPEF spectrum of $Au_{10\text{-}x}Ag_XSG_{10}$; x= 0-2 was also recorded. Interestingly, the TPEF spectrum of $Au_{10\text{-}X}Ag_XSG_{10}$ nanocluster (x= 0-2) showed less pronounced bathochromic shift in comparison to $Au_{10\text{-}x}Ag_XSG_{10}$; x = 1-4 (**Figure S5**). In addition, the absolute TPEF cross section of $Au_{10-x}Ag_xSG_{10}$ with x= 1-4 was measured to be 0.0024±0.0016 GM (780 nm laser excitation). Also, the effect of chemical substitution by silver doping on the first hyperpolarizability (β) value of $Au_{10}SG_{10}$ was evaluated. Intriguingly, as opposed to a high β value of $85(9) \times 10^{-30}$ esu for $Au_{10}SG_{10}$, a much reduced hyperpolarizability value of $14(6) \times 10^{-30}$ esu is found for $Au_{10-x}Ag_xSG_{10}$ with x= 1-4, see **Figure S6 in SI**.

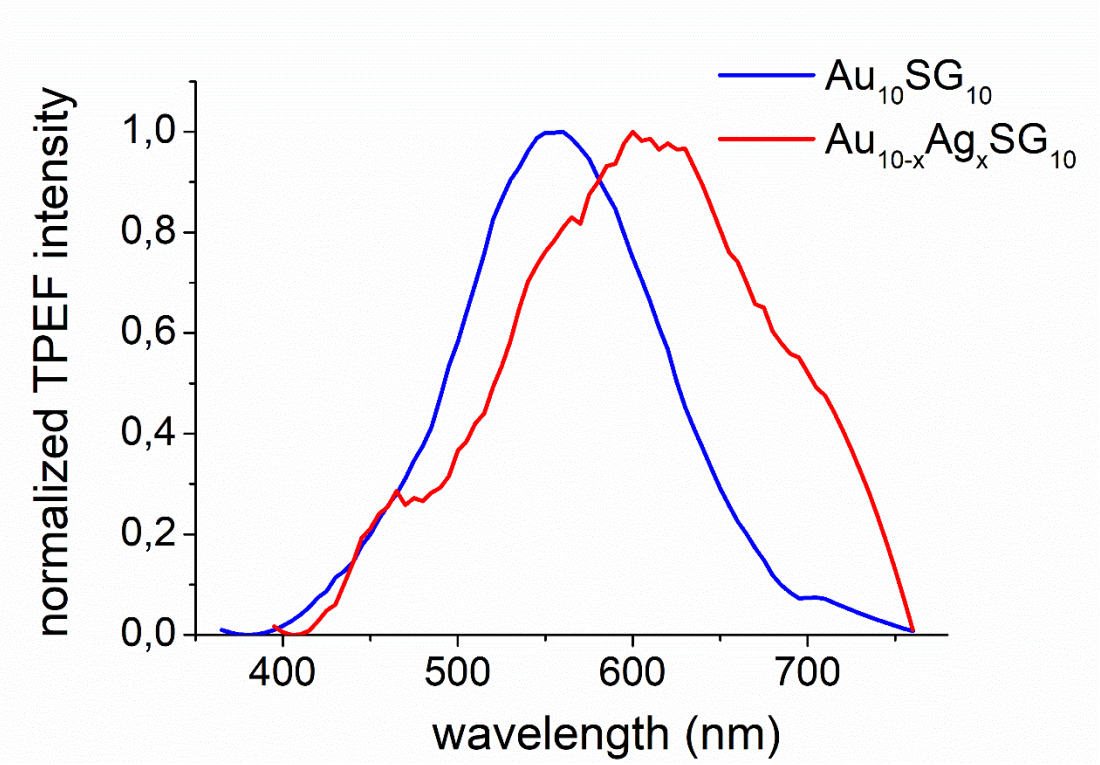

Figure 2: Normalized two-photon excited fluorescence spectra at excitation wavelength 780 nm of $Au_{10}SG_{10}$ compared to silver doped $Au_{10-x}Ag_xSG_{10}$ (x=1-4) in gels with the same concentration ~750 µM. TPEF measurements were performed on nanoclusters-containing gels with a customized confocal microscope.

An important question concerns the preservation of the catenane structure upon silver doping. In order to gain an insight into the structural property of the as-synthesized $Au_{10}SG_{10}$ and those doped with silver atoms, structural X-ray powder diffraction (XRPD) analysis was conducted, see **Figure S7** in SI. For pure Au_{10} nanoclusters, three possible isomers, namely [5,5] and [6,4] catenanes and the crown like structure, have been found as the lowest-energy structures, see **Figure S7**. Among these isomeric structures, the preserved [5,5] catenane structure has been found to be the lowest energy one for both Au_9AgSG_{10} and $Au_7Ag_3SG_{10}$, (SG has been replaced by SCH_3). Silver doping was found to have no significant effect on the global structure, bond lengths and bond angles, of the catenane rings. In doped isomers, the silver atoms are located at the center of the catenane structure, as shown in **Figure 3**. With computation of the XRPD pattern of *Au_9AgSG_{10}*

and $Au_7Ag_3SG_{10}$, the best agreement is obtained for the [5,5] catenane structure preserved upon doping with silver atoms, see **Figure S7**. The one photon absorption (OPA) spectra calculated using a TDDFT approach for the lowest-energy [5,5] catenane structures for $Au_{10}SG_{10}$, Au_9AgSG_{10} and $Au_7Ag_3SG_{10}$ is shown in **Figure 3A)** with a chiral $-SCH_2CH(NH_2)CH_3$ ligand as a model for glutathione. The first excited states involved in OPA are located between 360 and 330 nm. The leading excitations responsible for the excitation of the S_1 state are shown also in **Figure 3A)** and involve s to p excitation located on the gold atoms, s to p excitation located on the Ag and Au atoms and s to s excitation located on the Ag atoms for the pure Au, the Ag doped and the Ag_3 doped ligated clusters, respectively. A blue-shift of the S_1 state has been observed as a function of the number of silver atoms doped in the catenane structure. This blue-shift originates from a larger s to d gap in silver atoms due to smaller relativistic effects with respect to the gold atoms. The comparison with the measured features, and in particular the blue-shift in the absorption spectrum, confirms that the catenane structure remains preserved upon silver doping. Similar blue shifted chiroptical features for the $Au_7Ag_3SG_{10}$ system compared with $Au_{10}SG_{10}$ have been also found for the calculated CD spectra with the chiral ligand $-SCH_2CH(NH_2)CH_3$, as shown in **Figure S8 in SI**.

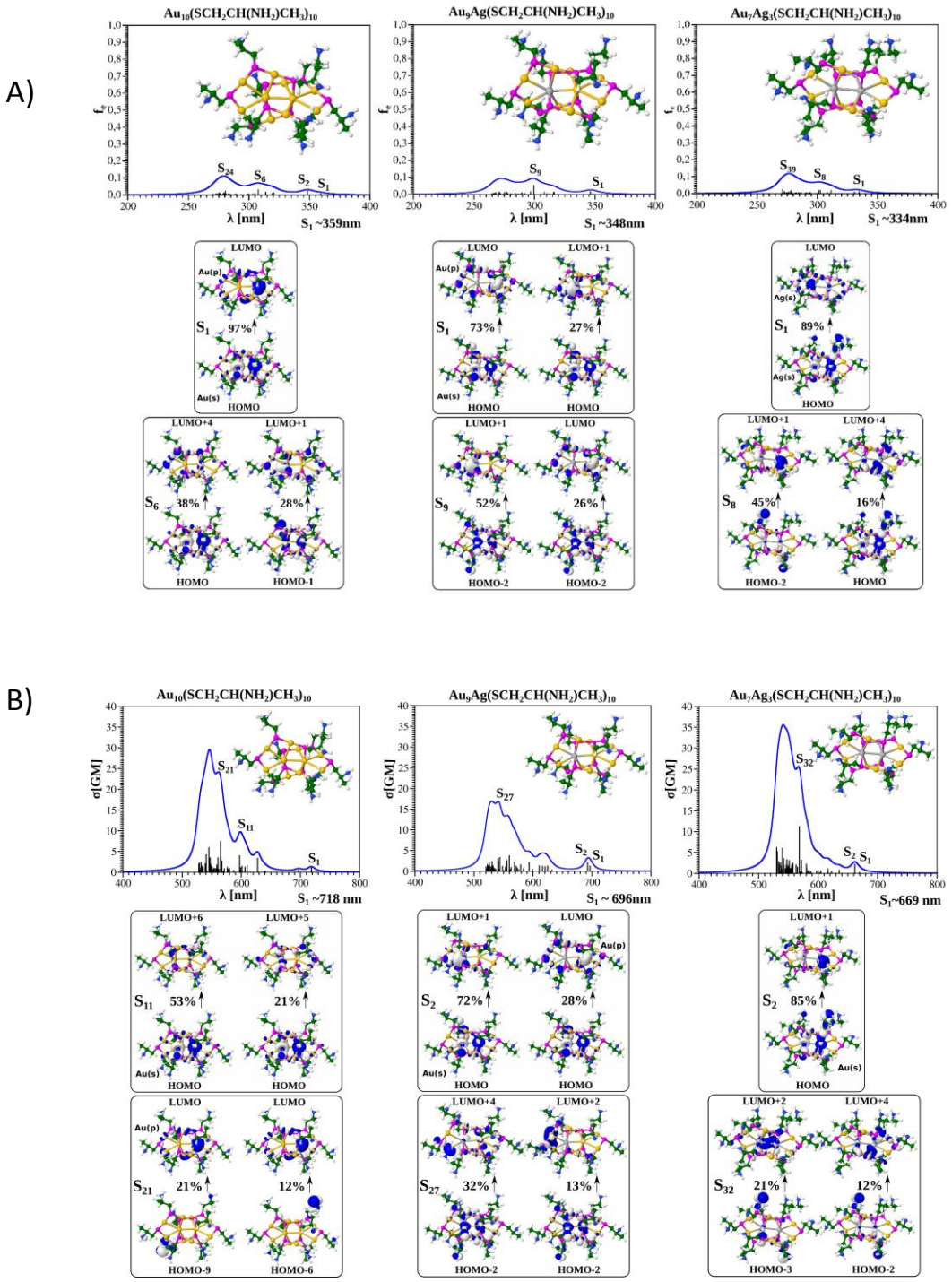

Figure 3: A) TD-DFT OPA spectrum for $Au_{10}L_{10}$, Au_9AgL_{10} $Au_7Ag_3L_{10}$ nanoclusters (with the chiral ligand ($-SCH_2CH(NH_2)CH_3$) for the lowest energy [5,5] catenane. Leading excitations responsible for the characteristic features of OPA are shown in bottom panels. B) TD-DFT TPA spectrum for $Au_{10}L_{10}$, Au_9AgL_{10} $Au_7Ag_3L_{10}$ nanoclusters (with the chiral ligand ($-SCH_2CH(NH_2)CH_3$) for the lowest energy [5,5] catenane. Leading excitations responsible for the characteristic features of TPA are shown in bottom panels.

A strong decrease of the first hyperpolarizability β for an excitation wavelength of 800 nm was observed upon silver doping. Two effects might explain this decrease: (i) structural changes of the Ag-doped $Au_{10}SG_{10}$ nanoclusters into more symmetrical structures (since second harmonic generation is only allowed for non-centrosymmetric structures) as compared to undoped nanoclusters and/or (ii) resonance effects between OPA and TPA states.[11, 43] Since we have confirmed previously that catenane structures remain preserved upon silver doping, hypothesis (i) can be excluded, although the exact position of silver atoms in the catenane structure may affect the symmetry of the structure. Furthermore, the calculated first hyperpolarizabilities β for the [5,5] catenane structure, see **Table S1** in SI for $Au_{10}SG_{10}$, Au_9AgSG_{10} and $Au_7Ag_3SG_{10}$ are in good agreement with the experimental values. Consequently, the decrease in hyperpolarizability of $Au_{10}SG_{10}$ upon silver doping is rather attributed to resonance effects. Due to blue shifted S_1 states, the resonance with S_1 state is not more efficient for $Au_7Ag_3SG_{10}$ in contrast to $Au_{10}SG_{10}$, as illustrated for two-photon absorption (TPA) spectra calculated using a TDDFT approach for the lowest-energy [5,5] catenane structures for $Au_{10}SG_{10}$, Au_9AgSG_{10} and $Au_7Ag_3SG_{10}$ in **Figure 3B**. It is worth mentioning that first hyperpolarizability β for silver doped Au nanoclusters should increase as illustrated for an excitation wavelength of 700 nm (see **Table S1** in SI).

Finally, one of the most significant effects of silver doping on the nonlinear optical properties of the clusters is the prominent bathochromic shift in the TPEF emission spectra. The red shift of ~ 50 nm in the TPEF spectrum of $Au_{10-x}Ag_xSG_{10}$ (x=1-4) may stem from altered relaxation of the S_1 first excited state of silver doped gold clusters as opposed to $Au_{10}SG_{10}$. A plausible mechanism interpreting the red shift in the TPEF emission spectrum of $Au_{10-x}Ag_xSG_{10}$ (x=1-4), in comparison to $Au_{10}SG_{10}$, has been proposed based on significantly different magnitude in relaxation of S_1 state upon silver doping, see **Figure 4**. In summary, doping by silver atoms does not influence OPA

spectra whereas the TPA cross section is slightly increased by three silver atoms doping. In contrast, the minimum of the S_1 state is lowered by approximately 1.5 eV for three silver atoms doping with respect of pure gold ligated cluster for which the lowering of the S_1 state is only 0.21 eV. The reason for the different lowering energies is the breaking of the silver-gold bonds in the first excited state of the three silver atoms doped clusters, see **Figure 4**.

This means that in addition to silver doping, the structural properties play the important role determining TPEF properties. For large cluster sizes the metallic core is formed in which doping by Ag atoms contributes to delocalized electrons of Au core. Therefore, in these cases smaller bathochromic shift in the TPEF emission spectra can be expected than in the case of catenane structure containing more directional metallic bonds. In fact, strong influence of Ag doping on nonlinear optical properties has been also shown for silver doped gold-cysteine supramolecular assemblies which contain directional metallic bonds.[9]

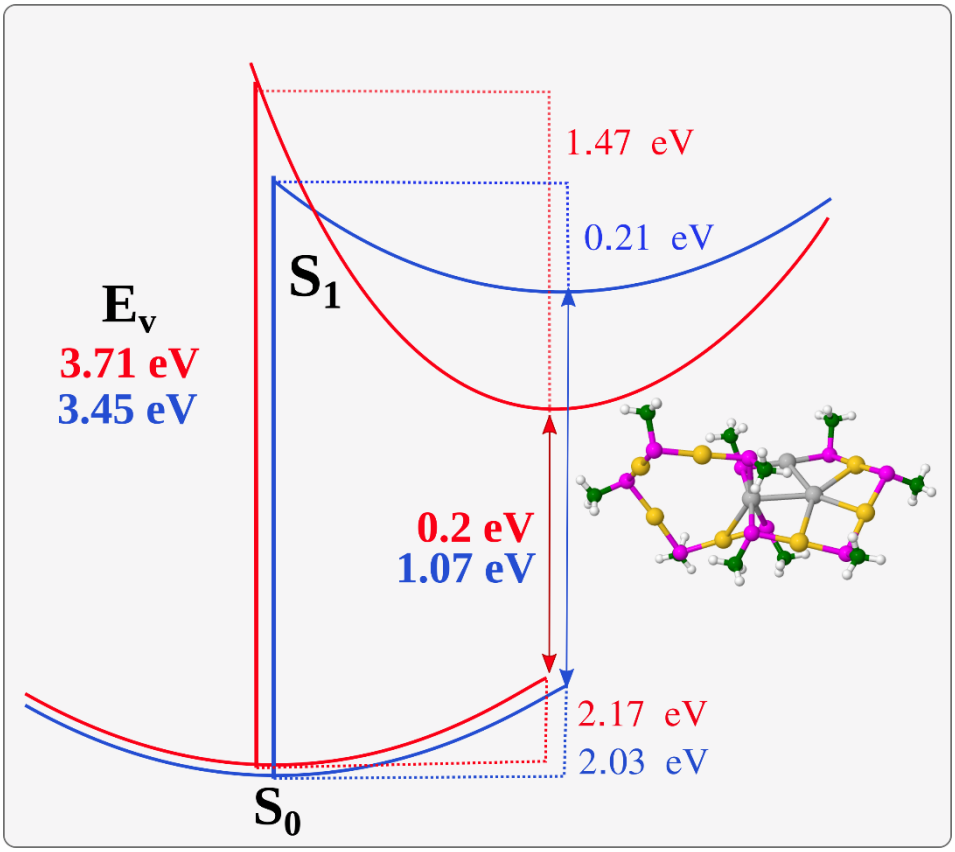

Figure 4: Calculated relaxation of the first excited state S1 of pure gold ligated cluster (blue) versus three silver atoms doped ligated cluster (red) with corresponding structure.

Conclusions

In summary, we report a rationale chemical strategy for the substitution of heteroatoms to alter the nonlinear optical properties of clusters with catenane structures. Notably, the strategy developed herein allows the fine-tuning of the multiphoton excitation properties, preserving the structure of the nanoclusters intact. This is important, given the wide utility of catenane like structures in catalysis and in molecular mechanics with molecular rotors. Furthermore, the experimental findings on the variation of the structure guided optical properties of the clusters, as a function of the number of doped heteroatoms, has been confirmed based on first principle theoretical calculations. In particular, the observed blue shift in the spectra is due to the larger s-d gap of Ag

atoms because of smaller relativistic effects as compared to the case of Au atom. The difference between the TPEF spectra is due to the Ag-Au bond breaking in the S_1 state, absent in the case of the Au-Au bond. Facile and robust chemical strategy allowing alteration of the absorption/emission characteristics of atomic clusters can serve as future key-point for fine tuning of nanoclusters applications.

Supporting Information. ESI-MS spectra of nanoclusters. Two-photon excited fluorescence spectra at excitation wavelength 780 nm of nanoclusters in gels. HRS line intensity of nanoclusters in aqueous solutions. Experimental and calculated XRD patterns of nanoclusters. DFT calculated CD spectra of the pure gold ligated cluster and silver-doped one. DFT calculated first hyperpolarizabilities for pure gold and silver doped ligated clusters at different wavelengths.

ACKNOWLEDGMENT

This research was partially supported by the project STIM-REI, Contract Number: KK.01.1.1.01.0003, funded by the European Union through the European Regional Development Fund – the Operational Programme Competitiveness and Cohesion 2014–2020 (KK.01.1.1.01). VBK, MPB and HF acknowledge computational facilities of the HPC computer within the STIM-REI project, Doctoral study of Biophysics at University of Split as well as Prof. Miroslav Radman at MedILS and Split-Dalmatia County for support. We would also like to acknowledge the financial support received from the French-Croatian project “International Laboratory for Nano Clusters and Biological Aging, LIA NCBA”.

REFERENCES

1. Antoine, R., Supramolecular Gold Chemistry: From Atomically Precise Thiolate-Protected Gold Nanoclusters to Gold-Thiolate Nanostructures. *Nanomaterials* **2020**, *10*, 377.
2. Goldmann, C.; Lazzari, R.; Paquez, X.; Boissière, C.; Ribot, F.; Sanchez, C.; Chanéac, C.; Portehault, D., Charge Transfer at Hybrid Interfaces: Plasmonics of Aromatic Thiol-Capped Gold Nanoparticles. *ACS Nano* **2015**, *9*, 7572-7582.
3. Jin, R.; Zeng, C.; Zhou, M.; Chen, Y., Atomically Precise Colloidal Metal Nanoclusters and Nanoparticles: Fundamentals and Opportunities. *Chem. Rev.* **2016**, *116*, 10346-10413.
4. Veselska, O.; Demessence, A., D10 Coinage Metal Organic Chalcogenolates: From Oligomers to Coordination Polymers. *Coord. Chem. Rev.* **2018**, *355*, 240-270.
5. Ungor, D.; Dékány, I.; Csapó, E., Reduction of Tetrachloroaurate(III) Ions with Bioligands: Role of the Thiol and Amine Functional Groups on the Structure and Optical Features of Gold Nanohybrid Systems. *Nanomaterials* **2019**, *9*, 1229.
6. Wu, Z.; Jin, R., On the Ligand's Role in the Fluorescence of Gold Nanoclusters. *Nano Lett.* **2010**, *10*, 2568-2573.
7. Kang, X.; Zhu, M., Tailoring the Photoluminescence of Atomically Precise Nanoclusters. *Chem. Soc. Rev.* **2019**, *48*, 2422-2457.
8. Jin, R.; Nobusada, K., Doping and Alloying in Atomically Precise Gold Nanoparticles. *Nano Res.* **2014**, *7*, 285-300.
9. Fakhouri, H.; Perić, M.; Bertorelle, F.; Dugourd, P.; Dagany, X.; Russier-Antoine, I.; Brevet, P.-F.; Bonačić-Koutecký, V.; Antoine, R., Sub-100 Nanometer Silver Doped Gold–Cysteine Supramolecular Assemblies with Enhanced Nonlinear Optical Properties. *Phys. Chem. Chem. Phys.* **2019**, *21*, 12091-12099.
10. Olesiak-Banska, J.; Waszkielewicz, M.; Obstarczyk, P.; Samoc, M., Two-Photon Absorption and Photoluminescence of Colloidal Gold Nanoparticles and Nanoclusters. *Chem. Soc. Rev.* **2019**, *48*, 4087-4117.
11. Bonačić-Koutecký, V.; Antoine, R., Enhanced Two-Photon Absorption of Ligated Silver and Gold Nanoclusters: Theoretical and Experimental Assessments. *Nanoscale* **2019**, *11*, 12436-12448.
12. Brach, K.; Waszkielewicz, M.; Olesiak-Banska, J.; Samoc, M.; Matczyszyn, K., Two-Photon Imaging of 3d Organization of Bimetallic Auag Nanoclusters in DNA Matrix. *Langmuir* **2017**, *33*, 8993-8999.
13. Brach, K.; Olesiak-Banska, J.; Waszkielewicz, M.; Samoc, M.; Matczyszyn, K., DNA Liquid Crystals Doped with Auag Nanoclusters: One-Photon and Two-Photon Imaging. *J. Mol. Liq.* **2018**, *259*, 82-87.
14. Van Steerteghem, N.; Van Cleuvenbergen, S.; Deckers, S.; Kumara, C.; Dass, A.; Häkkinen, H.; Clays, K.; Verbiest, T.; Knoppe, S., Symmetry Breaking in Ligand-Protected Gold Clusters Probed by Nonlinear Optics. *Nanoscale* **2016**, *8*, 12123-12127.
15. Guidez, E. B.; Mäkinen, V.; Häkkinen, H.; Aikens, C. M., Effects of Silver Doping on the Geometric and Electronic Structure and Optical Absorption Spectra of the Au25–Nagn(Sh)18– (N = 1, 2, 4, 6, 8, 10, 12) Bimetallic Nanoclusters. *J. Phys. Chem. C* **2012**, *116*, 20617-20624.

16. Liu, S., Single-Atom Doping on Thiolate-Protected Gold Nanoclusters: A Tddft Study on the Excited States. *Mater. Res. Express* **2019**, *6*, 1150g3.
17. Muniz-Miranda, F.; Menziani, M. C.; Pedone, A., Influence of Silver Doping on the Photoluminescence of Protected Agnau25–N Nanoclusters: A Time-Dependent Density Functional Theory Investigation. *J. Phys. Chem. C* **2015**, *119*, 10766-10775.
18. Xie, X.-Y.; Xiao, P.; Cao, X.; Fang, W.-H.; Cui, G.; Dolg, M., The Origin of the Photoluminescence Enhancement of Gold-Doped Silver Nanoclusters: The Importance of Relativistic Effects and Heteronuclear Gold–Silver Bonds. *Angew. Chem. Int. Ed.* **2018**, *57*, 9965-9969.
19. Wang, S.; Meng, X.; Das, A.; Li, T.; Song, Y.; Cao, T.; Zhu, X.; Zhu, M.; Jin, R., A 200-Fold Quantum Yield Boost in the Photoluminescence of Silver-Doped Agxau25−X Nanoclusters: The 13 Th Silver Atom Matters. *Angew. Chem. Int. Ed.* **2014**, *53*, 2376-2380.
20. van der Linden, M.; van Bunningen, A. J.; Amidani, L.; Bransen, M.; Elnaggar, H.; Glatzel, P.; Meijerink, A.; de Groot, F. M. F., Single Au Atom Doping of Silver Nanoclusters. *ACS Nano* **2018**, *12*, 12751-12760.
21. Comby-Zerbino, C.; Perić, M.; Bertorelle, F.; Chirot, F.; Dugourd, P.; Bonačić-Koutecký, V.; Antoine, R., Catenane Structures of Homoleptic Thioglycolic Acid-Protected Gold Nanoclusters Evidenced by Ion Mobility-Mass Spectrometry and Dft Calculations. *Nanomaterials* **2019**, *9*, 457.
22. Bertorelle, F.; Russier-Antoine, I.; Calin, N.; Comby-Zerbino, C.; Bensalah-Ledoux, A.; Guy, S.; Dugourd, P.; Brevet, P.-F.; Sanader, Ž.; Krstić, M.; et al., Au10(SG)10: A Chiral Gold Catenane Nanocluster with Zero Confined Electrons. Optical Properties and First-Principles Theoretical Analysis. *J. Phys. Chem. Lett.* **2017**, *8*, 1979-1985.
23. Comby-Zerbino, C.; Bertorelle, F.; Chirot, F.; Dugourd, P.; Antoine, R., Structural Insights into Glutathione-Protected Gold Au10−12(SG)10−12 Nanoclusters Revealed by Ion Mobility Mass Spectrometry. *Eur. Phys. J. D* **2018**, *72*, 144.
24. Russier-Antoine, I.; Bertorelle, F.; Calin, N.; Sanader, Z.; Krstic, M.; Comby-Zerbino, C.; Dugourd, P.; Brevet, P.-F.; Bonacic-Koutecky, V.; Antoine, R., Ligand-Core Nlo-Phores: A Combined Experimental and Theoretical Approach to the Two-Photon Absorption and Two-Photon Excited Emission Properties of Small-Ligated Silver Nanoclusters. *Nanoscale* **2017**, *9*, 1221-1228
25. Russier-Antoine, I.; Bertorelle, F.; Vojkovic, M.; Rayane, D.; Salmon, E.; Jonin, C.; Dugourd, P.; Antoine, R.; Brevet, P.-F., Non-Linear Optical Properties of Gold Quantum Clusters. The Smaller the Better. *Nanoscale* **2014**, *6*, 13572-13578.
26. Becke, A. D., Density-Functional Exchange-Energy Approximation with Correct Asymptotic-Behavior. *Phys. Rev. A* **1988**, *38*, 3098-3100.
27. Becke, A. D., A New Mixing of Hartree-Fock and Local Density-Functional Theories. *J. Chem. Phys.* **1993**, *98*, 1372-1377.
28. Lee, C. T.; Yang, W. T.; Parr, R. G., Development of the Colle-Salvetti Correlation-Energy Formula into a Functional of the Electron Density. *Phys Rev. B* **1988**, *37*, 785-789.
29. Weigend, F.; Ahlrichs, R., Balanced Basis Sets of Split Valence, Triple Zeta Valence and Quadruple Zeta Valence Quality for H to Rn: Design and Assessment of Accuracy. *Phys. Chem. Chem. Phys.* **2005**, *7*, 3297-3305.
30. V7.4, T. *A Development of University of Karlsruhe and Forschungszentrum Karlsruhe Gmbh, 1989-2007, Turbomole Gmbh, since 2007; Available from http://www.Turbomole.Com*

2019.

31. Bertorelle, F.; Hamouda, R.; Rayane, D.; Broyer, M.; Antoine, R.; Dugourd, P.; Gell, L.; Kulesza, A.; Mitric, R.; Bonacic-Koutecky, V., Synthesis, Characterization and Optical Properties of Low Nuclearity Liganded Silver Clusters: Ag31(SG)19 and Ag15(SG)11. *Nanoscale* **2013**, *5*, 5637-5643.
32. Bonacic-Koutecky, V.; Kulesza, A.; Gell, L.; Mitric, R.; Antoine, R.; Bertorelle, F.; Hamouda, R.; Rayane, D.; Broyer, M.; Tabarin, T.; et al., Silver cluster-biomolecule hybrids: from basics towards sensors. Phys. Chem. Chem. Phys. **2012**, 14, 9282-9290.
33. List, N. H.; Zaleśny, R.; Murugan, N. A.; Kongsted, J.; Bartkowiak, W.; Ågren, H., Relation between Nonlinear Optical Properties of Push–Pull Molecules and Metric of Charge Transfer Excitations. *Journal of Chemical Theory and Computation* **2015**, *11*, 4182-4188.
34. Norman, P., A Perspective on Nonresonant and Resonant Electronic Response Theory for Time-Dependent Molecular Properties. *Physical Chemistry Chemical Physics* **2011**, *13*, 20519-20535.
35. *Dalton, a Molecular Electronic Structure Program, Release Dalton2016. (2015), See http://daltonprogram.Org.* .
36. Aidas, K.; Angeli, C.; Bak, K. L.; Bakken, V.; Bast, R.; Boman, L.; Christiansen, O.; Cimiraglia, R.; Coriani, S.; Dahle, P.; et al. The Dalton quantum chemistry program system. *WIREs Computational Molecular Science*. **2014**, *4*, 269-284.
37. Rassolov, V. A.; Pople, J. A.; Ratner, M. A.; Windus, T. L., 6-31g* Basis Set for Atoms K through Zn. *J. Chem. Phys.* **1998**, *109*, 1223-1229.
38. Francl, M. M.; Pietro, W. J.; Hehre, W. J.; Binkley, J. S.; Gordon, M. S.; DeFrees, D. J.; Pople, J. A., Self- Consistent Molecular Orbital Methods. Xxiii. A Polarization- Type Basis Set for Second- Row Elements. *J. Chem. Phys.* **1982**, *77*, 3654-3665.
39. Dill, J. D.; Pople, J. A., Self- Consistent Molecular Orbital Methods. Xv. Extended Gaussian- Type Basis Sets for Lithium, Beryllium, and Boron. *J. Chem. Phys.* **1975**, *62*, 2921-2923.
40. Hehre, W. J.; Ditchfield, R.; Pople, J. A., Self—Consistent Molecular Orbital Methods. Xii. Further Extensions of Gaussian—Type Basis Sets for Use in Molecular Orbital Studies of Organic Molecules. *J. Chem. Phys.* **1972**, *56*, 2257-2261.
41. Andrae, D.; Haeussermann, U.; Dolg, M.; Stoll, H.; Preuss, H., Energy-Adjusted Ab Initio Pseudopotentials for the Second and Third Row Transition Elements. *Theor. Chim. Acta* **1990**, *77*, 123.
42. Guinier, A., *X-Ray Diffraction in Crystals, Imperfect Crystals, and Amorphous Bodies*; W.H. Freeman: San Francisco, 1963.
43. Hu, Z.; Jensen, L., Importance of Double-Resonance Effects in Two-Photon Absorption Properties of Au25(Sr)18−. *Chem. Sci.* **2017**, *8*, 4595-4601.

TOC GRAPHIC

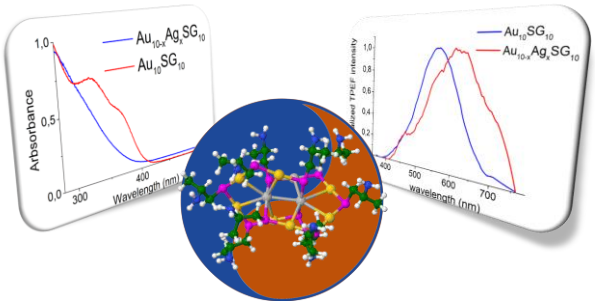
Au10-xAgxSG10
Au10SG10
Absorbance
1,0
0,5
0,0
300
400
Wavelength (nm)
Au10SG10
Au10-xAgxSG10
1,0
0,8
0,6
0,4
0,2
400
500
600
700
wavelength (nm)